

## CHARACTERIZATION OF PERFECTLY CONDUCTING TARGETS IN RESONANCE DOMAIN WITH THEIR QUALITY OF RESONANCE

J. Chauveau, N. de Beaucoudrey, and J. Saillard

Institut de Recherche en Electrotechnique  
et Electronique de Nantes Atlantique (IREENA)  
Université de Nantes  
Polytech'Nantes, rue Christian Pauc, BP50609  
44306 Nantes Cedex 03, France

**Abstract**—In resonance domain, the radar scattering response of any object can be modelled by natural poles of resonance with the formalism of the Singularity Expansion Method. The mapping of these poles in the complex plane gives useful information for the discrimination of a radar target, as its general shape, its characteristic dimension and its constitution. In this paper, we use an analogy with resonant circuits modelling to define the quality factor  $Q$  of each resonance. Therefore, we propose to characterize the resonance behavior of perfectly conducting targets with this quality factor  $Q$  and the natural pulsation of resonance  $\omega_0$ . Indeed, this new representation in  $\{\omega_0; Q\}$  allows to better separate information than the usual mapping of natural poles of resonance in the complex plane. For perfectly conducting canonical and complex shape targets, we present results exhibiting advantages of these two parameters  $\{\omega_0; Q\}$ .

### 1. INTRODUCTION

For years, the Singularity Expansion Method (SEM) has been used to characterize the electromagnetic response of structures in both the time and the frequency domains. SEM was first introduced by Baum [1, 2] and was inspired by observing that typical transient temporal responses of various scatterers (e.g. aircrafts, antennas, ...) behave as a combination of exponentially damped sinusoids. Such damped sinusoids correspond, in the complex frequency domain, to complex conjugate poles called natural poles of resonance. The knowledge of these singularities is an useful information for the discrimination

of radar targets and it has been used for different purposes of discrimination and identification [3–6]. In fact, the mapping of these natural poles in cartesian complex plane behaves as an identity card allowing to recognize the detected target by comparison with a library of mapping of poles, created before experiments for a set of possible targets. Thus, the information contained in poles of resonance can give some indications on the general shape, the nature and the constitution of the illuminated target.

We propose here to compare resonance phenomena of targets with RLC resonant circuits. Indeed, both scatterers and RLC resonators can be analysed in terms of their poles pattern in the complex frequency plane. From this comparison, we define the quality factor of each resonance of the target. The quality factor is an important parameter which allows to estimate the selectivity of resonance of a system. Accordingly, we propose to use a new representation with the natural pulsation of resonance and the quality factor. Indeed, it is very interesting to classify radar targets as a function of their resonant behavior and this new representation allows to better separate informations.

First, in Section 2, we briefly introduce the resonance poles. Then, in Section 3, we use the comparison of resonance phenomena of targets with resonant circuits to define the quality factor  $Q$  and the natural pulsation of resonance  $\omega_0$  for each resonance of the target. Finally, we present results exhibiting advantages of this representation in  $\{\omega_0; Q\}$ , in Section 4.1, for several perfectly conducting (PC) canonical targets and, in Section 4.2, for a PC complex shape target.

## 2. RESONANCES POLES OF RADAR TARGETS

A radar target is illuminated in the far field region by an incident broadband signal including the resonance domain of the target. The resonance domain corresponds to electromagnetic wavelengths of the same order as object dimensions. In this frequency band, the fluctuation of the energy scattered by the target is significant, with induced resonances occurring at particular frequencies. In the time domain, the scattered transient response is composed of two successive parts. First, the impulsive part,  $h_E(t)$ , corresponding to the early time, comes from the direct reflection of the incident wave on the object surface. In general, for a monostatic configuration, in free space, this forced part is of duration  $0 < t \leq 2D/c = T_L$ , where  $D$  is the greatest dimension of the target [8]. Next, during the late time ( $t \geq T_L$ ), the oscillating part,  $h_L(t)$ , is due to resonance phenomena of the target. These resonances have two origins [7]: resonances occurring outside

the object are called “external resonances” and correspond to surface creeping waves. Conversely, resonances occurring inside the object are called “internal resonances” and correspond to potential cavity waves. In the case of a perfectly conducting target, only external resonances occur. The resonant behavior during the late time is characteristic of the studied target and can be used to define a method of identification.

The Singularity Expansion Method (SEM) [1, 2] provides a convenient methodology, describing the late time response of various scatterers as a finite sum of exponentially damped sinusoids

$$h_L(t) \approx \sum_{m=1}^M 2 |R_m| \exp(\sigma_m(t)) \cos(\omega_m(t) + \phi_m) \quad (t \geq T_L) \quad (1)$$

Conversely, the Laplace transform of equation (1) gives the transfer function  $H(s)$  corresponding to the sum of pairs of complex conjugate poles in the complex frequency plane

$$H(s) \approx \sum_{m=1}^M \left( \frac{R_m}{s - s_m} + \frac{R_m^*}{s - s_m^*} \right) \quad (2)$$

where  $M$  is the total number of modes of the development,  $s$  is the complex variable in the Laplace plane. For the  $m^{th}$  singularity,  $R_m$  is the residue associated to each resonance pole  $s_m = \sigma_m + j\omega_m$  ( $R_m^*$  and  $s_m^*$  are complex conjugate of  $R_m$  and  $s_m$ ). The imaginary part,  $\omega_m$ , is the resonance pulsation. The real part,  $\sigma_m$ , is negative, indeed corresponding to a damping coefficient due to losses on the surface and, eventually, inside not perfectly conducting targets.

The interest for the characterization of targets led to the development of algorithms for finding resonance poles and their associated residues, using either the impulse response of targets in the time domain or their transfer function in the frequency domain [2, 9–18]. For our simulations, we can use any of existing methods of poles extraction. We choose a frequency domain method [8–13], because we get frequential data from an electromagnetic simulation software based on the Method of Moments [19].

As an example, we present in Fig. 1 the modulus of the transfer function  $H(\omega)$  of two perfectly conducting canonical targets: a dipole of length  $L = 0.10$  m and aspect-ratio  $L/D = 400$ , where  $D$  is its diameter, and a sphere with diameter  $D = 0.064$  m. These targets are studied in free-space, in the frequency range [1 GHz; 11 GHz] which contains the zone of resonance of the studied targets (the pulsation range is [ $\omega_{min} = 0.63 \cdot 10^{10}$  rad/sec;  $\omega_{max} = 6.9 \cdot 10^{10}$  rad/sec]). We specify that it is important to have *a priori* information on scatterer

dimensions to define the frequency range such as it really includes the searched poles of resonance [2]. Only poles with pulsation  $\omega_m$  included in the pulsation range  $[\omega_{min} ; \omega_{max}]$  can be extracted. We note that for a very resonant object, as the dipole, resonance peaks are narrow and clearly appear in the response  $|H(\omega)|$ , what is not the case for a less resonant object as the sphere.

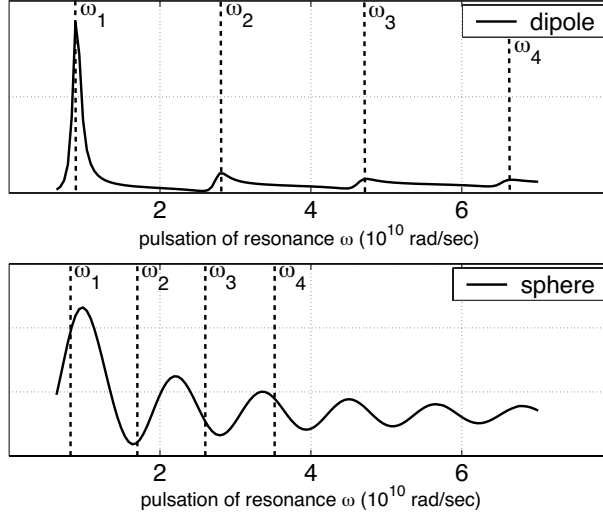


**Figure 1.** Modulus of the transfer function  $H(\omega)$  of the dipole (upper) and the sphere (lower) (monostatic configuration — 256 samples).

In order to extract poles of resonance, the frequential response,  $H$ , is approximated by a ratio of two complex polynomials [9–13]. The zeros of the denominator polynomial,  $B(s)$ , are the poles of  $H(s)$ . We get

$$H(s) \approx \frac{A(s)}{B(s)} \approx \sum_{n=1}^N \frac{R_n}{s - s_n} \quad (3)$$

where  $N$  is the total number of singularities of the development and  $R_n$  is the residue associated to each pole  $s_n$ . Among these  $N$  poles, we expect to get the  $2M$  physical poles corresponding to equation (2), called “natural” poles of resonance. They are complex conjugate by pair, with negative real part  $\sigma_m$ , and should be independent of the order  $N$  of the rational function. In fact, we find not only these natural poles of resonance but also parasitical poles, the ones which are not complex conjugate by pair and/or have a positive real part. Moreover, these parasitical poles depend of the order  $N$  in equation (3). To

be sure to get the whole set of natural poles of resonance existing in the studied frequency range, we choose a high value of the order  $N$  ( $N = 50$  for instance). In order to separate the  $2M$  natural poles of resonance and the  $N - 2M$  parasitical poles, we vary the value of  $N$  of some units ( $N = 50 \pm 2$ ). Consequently, the poles are natural ones not only if they are complex conjugate by pair and have a negative real part, but also if their value is stable when  $N$  varies (for instance:  $2M = 8$  for the studied dipole).

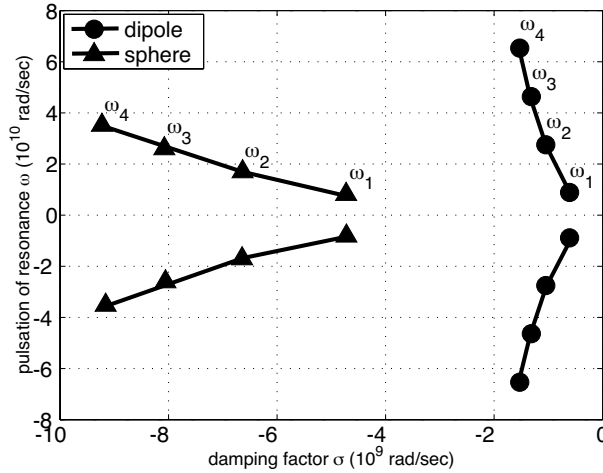


**Figure 2.** Mapping of natural poles of resonance extracted from  $H(\omega)$  of the dipole and the sphere, in the complex plane  $\{\omega; \sigma\}$ . ( $M = 4$ ).

Fig. 2 shows the mapping of natural poles of resonance for the studied targets, in the half complex plane because resonance poles have a negative real part ( $\sigma < 0$ ). Indeed, for canonical targets (sphere, cylinder, dipole ...), poles are distributed over branches joining the fundamental pulsation of resonance,  $\omega_1$ , and harmonic pulsations. For a very resonant target as a dipole, we can notice in Fig. 1 (upper) that resonance peaks of  $|H(\omega)|$  occur at pulsations of resonance  $\omega_m$  of resonance poles in Fig. 2. However, in the case of weakly resonant targets as the sphere, peaks of resonance, corresponding to pulsation of resonance,  $\omega_m$ , overlay and cannot be distinguished in the modulus of the transfer function  $|H(\omega)|$  (Fig. 1 (lower)). Indeed, low resonant targets have poles of resonance with high value of damping factor,  $|\sigma_m|$ , corresponding to wide peaks, and are close to each other. Moreover, because of this low resonant behavior, resonance poles of high order ( $s_m > s_4$  for the studied sphere) become difficult to

obtain. Only the fundamental pole of resonance and some harmonic poles can be obtained. On the contrary for the dipole, we can extract all the existing resonance poles (i.e. resonance poles with pulsation  $\omega_m$  included in the pulsation range  $[\omega_{min}; \omega_{max}]$ ).

The main advantage of using natural poles of resonance for the discrimination of targets is that only 3 parameters  $\{\omega_m; \sigma_m; R_m\}$  are required to define each resonance mode. Furthermore, in a homogeneous medium, the mapping of natural poles in the complex plane  $\{\omega_m; \sigma_m\}$  is independent of the target orientation relatively to the excitation [20].

### 3. COMPARISON WITH RESONANT CIRCUITS

Actually, it is interesting to compare such resonance phenomena of radar objects with *RLC* resonant circuits.

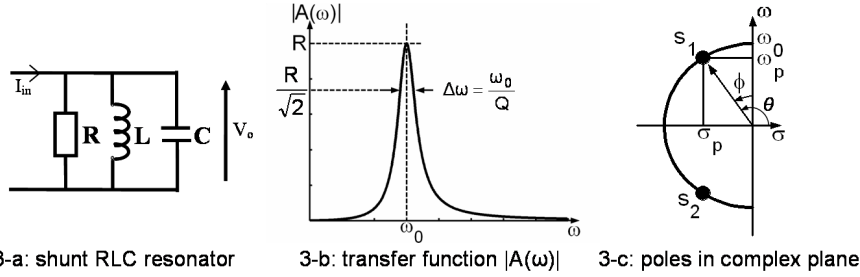


**Figure 3.** Example of a resonant circuit.

For example, the transfer function,  $A(\omega)$ , of the circuit of Fig. 3-a corresponds to the impedance,  $Z$ , given by (Fig. 3-b)

$$A(\omega) = Z(\omega) = \frac{V_0}{I_{in}} = \frac{R}{1 + jRC\omega + R/jL\omega} \quad (4)$$

The peak occurs at the natural pulsation of resonance  $\omega_0 = 1/\sqrt{LC}$ , with a bandwidth  $\Delta\omega = \omega_0/Q$ , where the quality factor is  $Q = RC\omega_0 = R/L\omega_0$ . Thus a narrow-band response gives a high  $Q$ .

If we replace the circuit component parameters,  $R$ ,  $L$ , and  $C$ , by the more general ones,  $Q$  and  $\omega_0$ , Eq. (4) becomes Eq. (5), valid for any resonator, mechanical as well as electrical,

$$A(\omega) = \frac{R}{1 + jQ \left( \frac{\omega}{\omega_0} - \frac{\omega_0}{\omega} \right)} \quad (5)$$

In order to determine the poles of such a resonator, we replace, in Eq. (5),  $j\omega$  by  $s$ , complex variable in the Laplace plane. Thus, the  $s$ -plane transfer function is

$$\begin{aligned} A(s) &= R \frac{s(\omega_0/Q)}{s^2 + s(\omega_0/Q) + \omega_0^2} \\ &= R \frac{\omega_0}{Q} \frac{s}{(s - s_1)(s - s_2)} = \frac{r_1}{(s - s_1)} + \frac{r_2}{(s - s_2)} \end{aligned} \quad (6)$$

with  $s_1$  and  $s_2$ , the two roots of the denominator of  $A(s)$

$$s_{1,2} = -\frac{\omega_0}{2Q} \pm j\omega_0 \sqrt{1 - \left(\frac{1}{2Q}\right)^2} \quad (7)$$

For  $Q > 1/2$ , the two poles  $s_{1,2}$  are complex conjugate, with respective residue  $r_{1,2}$

$$r_1 = r_2^* = R \frac{\omega_0}{Q} \frac{s_1}{(s_1 - s_2)} \quad (8)$$

In the complex plane (Fig. 3-c), the poles,  $s_{1,2} = \sigma_p \pm j\omega_p$ , are located on the half-circle of radius equal to the natural pulsation of resonance,  $\omega_0$ . The real part of poles,  $\sigma_p = -\frac{\omega_0}{2Q} = -\frac{\Delta\omega}{2}$ , is the damping factor and the imaginary part is the damped pulsation  $\omega_p = \omega_0 \sqrt{1 - \left(\frac{1}{2Q}\right)^2}$ .

When  $Q$  value is high,  $\omega_p$  is very close to  $\omega_0$ .

In polar coordinates, we get:  $s_{1,2} = \omega_0 \exp \pm i\theta$ , with  $\omega_0$  the modulus and  $\theta$  the angle of  $s_{1,2}$ . We prefer to use a modified polar representation in the half complex plane:  $\{\omega_0; \Phi\}$  where  $\Phi = \theta - \pi/2$  is the angle between the pole direction and the imaginary axis  $\omega$ . We have

$$2 \sin \Phi = -\frac{2\sigma_p}{\omega_0} = -\frac{\Delta\omega}{\omega_0} = \frac{1}{Q} \quad (9)$$

Indeed,  $\Phi$  is related to the relative selectivity (i.e. the width  $\Delta\omega$  of the peak of resonance (Fig. 3-b) divided by the pulsation of resonance  $\omega_0$ ) which is equal to  $1/Q$ . Thus, a high  $Q$  corresponds to a low  $\Phi$  and the associated pole is close to the vertical axis.

Finally, instead of using the cartesian representation of resonance poles in  $\{\sigma_p; \omega_p\}$ , it is interesting to use a new representation in  $\{\omega_0; Q\}$ .

Now, we apply this resonant circuit analogy to the scattering transfer function  $H(s)$  of radar targets (Eq. (2)), which can be expressed as a sum of transfer functions  $A_m(s)$  (Eq. (6)) of elementary resonators  $\{\omega_{0,m}; Q_m\}$ .

For the  $m^{\text{th}}$  singularity ( $s_m = \sigma_m + j\omega_m$ ), the natural pulsation of resonance,  $\omega_{0,m}$ , and the quality factor,  $Q_m$ , are respectively given by

$$\omega_{0,m} = |s_m| \quad Q_m = -\frac{\omega_{0,m}}{2\sigma_m} \quad (10)$$

#### 4. USE OF THE QUALITY FACTOR FOR THE CHARACTERIZATION OF PC OBJECTS

The quality factor is an important parameter specifying the selectivity of a resonant system. It is used for instance for antennas [21, 22]. On account of the previous analysis of resonators, we propose to use no longer the parameters  $\{\sigma_m; \omega_m\}$  but the parameters  $\{\omega_{0,m}; Q_m\}$  to characterize radar targets according to their resonant behavior. We first study several PC canonical objects (4.1), then a PC complex shape target (4.2).

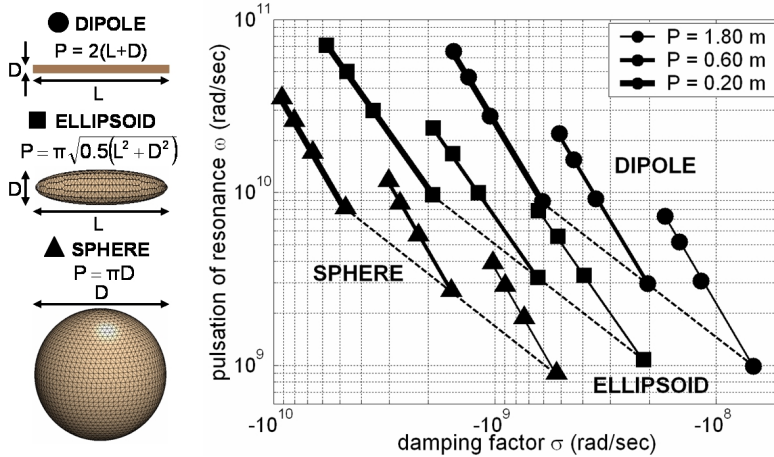


**Figure 4.** Mapping of resonance poles in  $\{\sigma_m; \omega_m\}$  for nine PC canonical targets: 3 dipoles ( $P$  variable;  $L/D = 400$ ), 3 ellipsoids ( $P$  variable;  $L/D = 8$ ), 3 spheres ( $P$  variable;  $L = D$ ). ( $L$ : Length;  $D$ : Diameter;  $P$ : Perimeter). Log-Log scale.

##### 4.1. PC Canonical Objects

Fig. 4 presents the usual mapping of resonance poles  $\{\sigma_m; \omega_m\}$  in the complex plane for nine PC canonical objects. Fig. 5 shows the evolution of the Q-factor,  $Q_m$ , as a function of the natural pulsation of resonance,  $\omega_{0,m}$ , for the same targets. It is interesting to observe

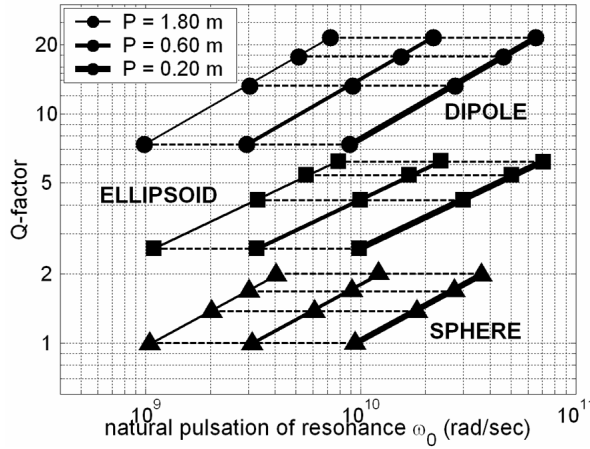


**Figure 5.** Evolution of Q-factor as a function of  $\omega_0$   $\{\omega_{0,m}; Q_m\}$  for the same PC canonical targets of Fig. 4. Log-Log scale.

that this representation in  $\{\omega_{0,m}; Q_m\}$  clearly brings out the resonance behavior of each target. Particularly, we can notice that the more objects are elongated, the more the Q-factor is high. Furthermore, for a same kind of object,  $Q$  is constant for the same aspect ratio,  $L/D$ , as indicated by horizontal dashed lines joining corresponding resonance poles (fundamental or harmonics) in Fig. 5. From equation 9, we can see that each value of  $Q$  corresponds to the same  $\Phi$  angle between the pole direction and the vertical axis in the linear mapping  $\{\sigma; \omega\}$  (Fig. 3-c). Consequently, poles located on a same horizontal line in Fig. 5 are located on a straight line passing through the origin, with slope  $a$  equal to

$$a = \frac{\omega_p}{\sigma_p} = \frac{1}{\tan \Phi} = \sqrt{4Q^2 - 1} \quad (11)$$

For a better visibility of poles, the Figure 4 is presented in log-log scale, consequently, this straight line of slope  $a$  is transform in straight line of slope 1 at vertical level equal to  $\text{Log}(a)$ . In Fig. 4, are plotted such dashed lines corresponding to fundamental poles of each kind of object.

Thus, the new representation of poles in  $\{\omega_{0,m}; Q_m\}$  allows to better separate informations and, consequently, to classify more efficiently radar targets as a function of their resonant behavior. Elongated targets correspond to a high  $Q$  value, while compact targets, having a higher surface for the same perimeter, correspond to a low  $Q$

value, because of higher radiating losses on the surface. Moreover,  $Q$  factor is lower in the case of targets with geometrical symmetries, on account of the degeneracy phenomenon of resonance poles [23].

In the same manner as a library of mapping of poles  $\{\sigma_p; \omega_p\}$ , it would be interesting to create a library of possible targets as a function of the  $\{\omega_{0,m}; Q_m\}$  representation.

#### 4.2. PC Complex Shape Target

A complex shape target can often be modeled as a combination of canonical objects (Fig. 6). Resonances occurring at particular frequencies correspond as well to canonical objects (here: cylinder, cone and three triangular wings) as to structures created by the assembly of these canonical objects (for instance: dihedral created by the junction between each triangle and the cylinder). However, among the whole set of these possible resonances, only a few of them appreciably contribute to the target response and are thus extracted [24]. As previously, extracted poles of resonances are distributed over some distinct branches joining the fundamental pulsation of resonance and corresponding harmonic pulsations.

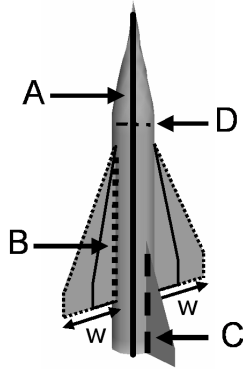


**Figure 6.** Example of a PC complex shape target.

Using the correspondence between pulsations of resonance and characteristic dimensions of an object, we associate these branches to elementary components of the complex shape target [25]. Indeed, creeping waves on the surface of a PC target are in resonance if their pulsation,  $\omega_{0,m}$ , corresponds to a characteristic dimension of the target such as its perimeter  $P = m\lambda_m = m\frac{2\pi c}{\omega_{0,m}}$ , with  $m = 1$  for the fundamental pulsation of resonance and,  $m > 1$  and integer, for harmonic pulsations. Fig. 7 showing the currents distribution on the surface of

the target excited with different pulsations of resonance, allows to illustrate the resonant behavior of the target. In Fig. 7(a), we can see that the pulsation  $\omega_0 = 0.57 \cdot 10^9$  rad/sec corresponds to the length of the target body ('A' in Fig. 6). In the same manner, we can see more distinctly in Fig. 7(b) that the pulsation  $\omega_0 = 1.32 \cdot 10^9$  rad/sec corresponds to dihedrals created by the junction between the two main wings and the body ('B' in Fig. 6), and in Fig. 7(c) that the pulsation  $\omega_0 = 1.86 \cdot 10^9$  rad/sec corresponds to the dihedral created by the junction between the little wing and the body ('C' in Fig. 6). Indeed, when the pulsation corresponds to the characteristic dimension of an elementary component of the target, currents are concentrated on this elementary component.

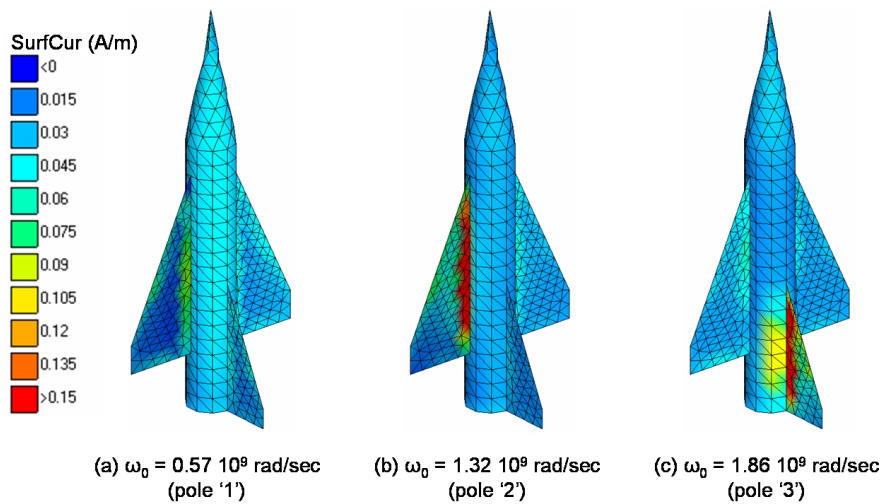


**Figure 7.** Surface currents on the PC complex shape target of Fig. 6 for 3 pulsations of resonance.

In order to clearly show how branches of poles are associated to elementary components of the target, we study the whole complex shape target (Fig. 6) and three partial complex shape targets: the target body alone in Fig. 8, the target body with the little wing in Fig. 9, and the target body with the two main wings in Fig. 10. These three figures present results comparing the whole target and each partial target, in both representations, the mapping of resonance poles  $\{\sigma_m; \omega_m\}$  and the representation in  $\{\omega_{0,m}; Q_m\}$ , both in linear scale.

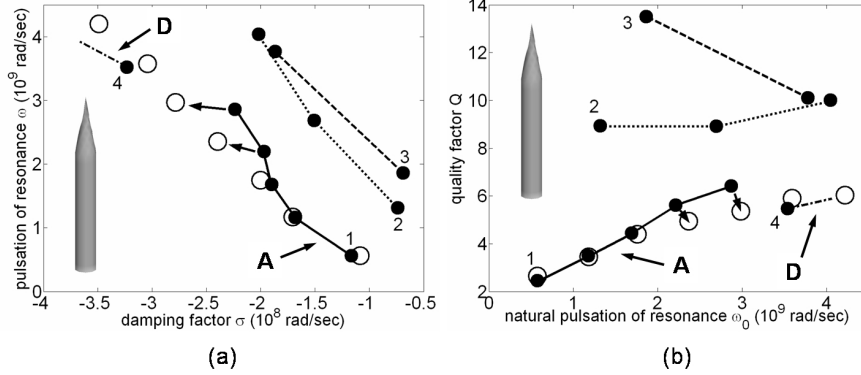


**Figure 8.** Comparison between the whole target (●) and the partial target (○) [target body alone]. (a)  $\{\sigma_m; \omega_m\}$ , (b)  $\{\omega_{0,m}; Q_m\}$ .

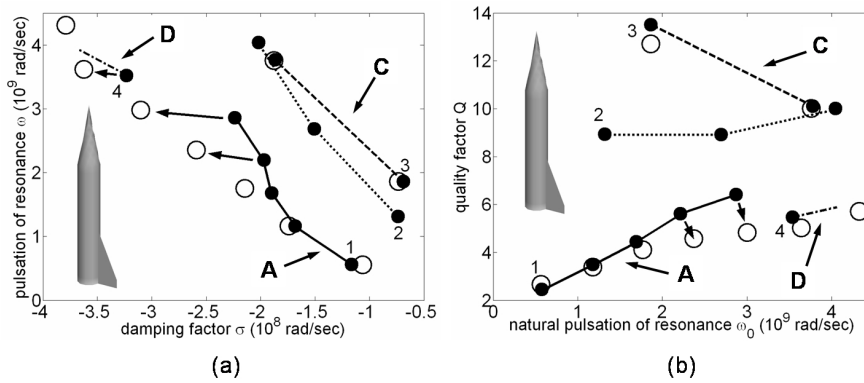


**Figure 9.** Comparison between the whole target (●) and the partial target (○) [target body + little wing]. (a)  $\{\sigma_m; \omega_m\}$ , (b)  $\{\omega_{0,m}; Q_m\}$ .

From Fig. 8, we can see that the branch named ‘A’, joining the fundamental pole ‘1’ and its harmonic poles, corresponds to the length of the body of the target, noted ‘A’ in Fig. 6. In the same way, the branch named ‘D’, with one pole ‘4’, corresponds to the circular section of the body, noted ‘D’ on Fig. 6. Next, results of Fig. 9 show that the ‘C’ branch, with fundamental pole ‘3’, actually corresponds to the dihedral created by the junction between the little wing and the body, noted ‘C’ in Fig. 6. Finally, results of Fig. 10 show that the ‘B’ branch, with fundamental pole ‘2’, actually corresponds to dihedrals created by the junction between the two main wings and the body, noted ‘B’ on Fig. 6.

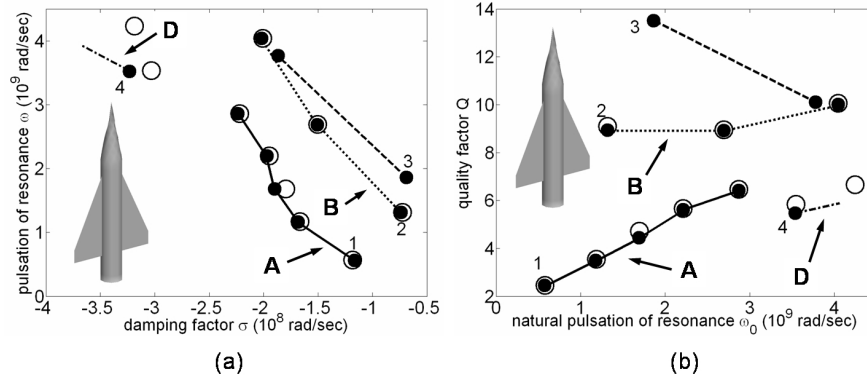


**Figure 10.** Comparison between the whole target (●) and the partial target (○) [target body + two wings]. (a)  $\{\sigma_m; \omega_m\}$ , (b)  $\{\omega_{0,m}; Q_m\}$ .

Poles of resonance corresponding to the target body (branches named ‘A’ and ‘D’) are present for the three partial targets. However, in Fig. 8 and 9, some harmonic poles of the ‘A’ branch are shifted, mainly in horizontal direction ( $\sigma$ ) in  $\{\sigma_m; \omega_m\}$  representation and in vertical direction ( $Q$ ) in  $\{\omega_{0,m}; Q_m\}$  representation. In fact, this poles shift comes from the coupling of canonical objects [26]. Poles of the ‘A’ branch are almost in the same location for the whole target and for the partial target in Fig. 10, because these two targets are nearly identical.

By using the representation in  $\{\omega_{0,m}; Q_m\}$ , it is easier to distinguish and to classify elementary components of the target from the quality of their resonance and from their natural pulsation of resonance. For example, in the case of the complex shape target of Fig. 6, results show that the ‘C’ branch, corresponding to the dihedral created by the junction between the little wing and the body, corresponds to the highest quality of resonance.

Furthermore, we propose to show that the representation in  $\{\omega_{0,m}; Q_m\}$  allows to better separate informations when a dimension of the target is varying. For this purpose we vary the size,  $w$ , of the two main wings (Fig. 6). Fig. 11 presents the mapping of resonance poles and the representation in  $\{\omega_{0,m}; Q_m\}$  for several values of  $w$ . ‘A’, ‘C’, and ‘D’ branches are in the same location. On the contrary, we can see that the ‘B’ branch, corresponding to the two main wings, moves as a function of  $w$ . the natural pulsation of resonance  $\omega_0$  is nearly constant, it is indeed a characteristic of the junction of the two main wings and the body. Only the Q-factor varies when  $w$  decreases, and thus the ‘B’ branch becomes increasingly resonant.

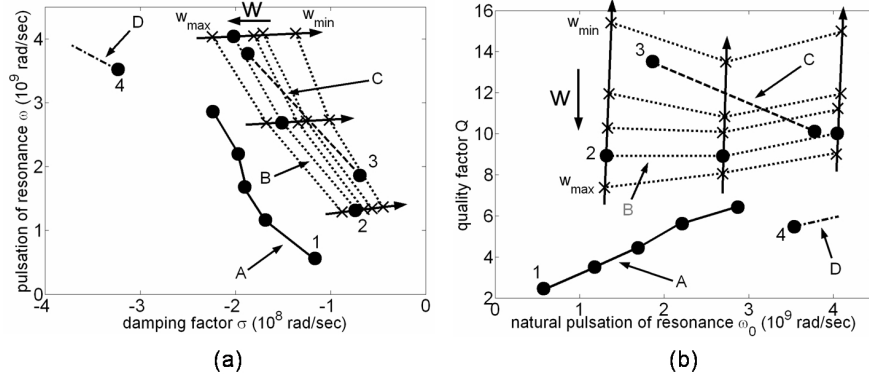


**Figure 11.** Evolution of resonance poles of the ‘B’ branch as a function of the wing width  $w$ .

## 5. CONCLUSION

In this paper, instead of using usual mapping of resonance poles in  $\{\sigma_m; \omega_m\}$ , we have proposed to characterize targets with the quality factor,  $Q$ , and the natural pulsation of resonance,  $\omega_0$ , defined by comparing resonance phenomena of targets to RLC resonant circuits. We have shown that this representation in  $\{\omega_{0,m}; Q_m\}$  allows to better separate informations: the  $Q$  parameter allows to bring out clearly the resonance behavior of targets and the natural pulsation of resonance,  $\omega_{0,m}$ , depends on dimensions of targets. Next, we have shown that each branch of poles corresponding to each elementary component of a perfectly conducting complex shape target moves as a function of dimensions of this elementary component. Here, we have presented results only for PC objects. It would be very interesting to extend this study to dielectric targets. Knowing that internal resonances have a damping factor much lower than external resonances, the quality factor will be much higher.

## REFERENCES

1. Baum, C. E., “The singularity expansion method,” *Transient Electromagnetic Field*, L. B. Felsen (ed.), 129–179, Springer-Verlag, New York, 1976.
2. Baum, C. E., E. J. Rothwell, K. M. Chen, and D. P. Nyquist, “The singularity expansion method and its application to target

- identification,” *Proceedings of the IEEE*, Vol. 79, No. 10, 1481–1492, October 1991.
3. Rothwell, E. J., K. M. Chen, and D. P. Nyquist, “Extraction of the natural frequencies of a radar target from a measured response using E-pulse techniques,” *IEEE Trans. Ant. Prop.*, Vol. 35, No. 6, 715–720, 1987.
  4. Chen, K. M., D. P. Nyquist, E. J. Rothwell, L. L. Webb, and B. Drachman, “Radar target discrimination by convolution of radar return with extinction-pulses and single-mode extraction signals,” *IEEE Trans. Ant. Prop.*, Vol. 34, No. 7, 896–904, 1986.
  5. Toribio, R., P. Pouliguen, and J. Saillard, “Identification of radar targets in resonance zone: E-pulse techniques,” *Progress In Electromagnetics Research*, PIER 43, 39–58, 2003
  6. Lee, J. H. and H. T. Kim, “Radar target discrimination using transient response reconstruction,” *Journal of Electromagnetic Waves and Applications*, Vol. 19, No. 5, 655–669, 2005.
  7. Chen, C-C., “Electromagnetic resonances of immersed dielectric spheres,” *IEEE Trans. Ant. Prop.*, Vol. 46, No. 7, 1074–1083, 1998.
  8. Kennaugh, E. M. and D. L. Moffatt, “Transient and impulse response approximations,” *Proceedings of the IEEE*, Vol. 53, 893–901, August 1965.
  9. Cauchy, A. L., “Sur la formule de Lagrange relative à l’interpolation,” *Analyse Algébrique*, Paris, 1821.
  10. Adve, R. S., T. K. Sarkar, S. M. Rao, E. K. Miller, and D. R. Pflug, “Application of the Cauchy method for extrapolating/interpolating narrow-band system responses,” *IEEE Trans. Mic. Theory and Tech.*, Vol. 45, No. 5, 837–845, 1997.
  11. Tesche, F. M., “On the analysis of scattering and antenna problems using the singularity expansion technique,” *IEEE Trans. Ant. Prop.*, Vol. 21, No. 1, 53–62, 1973.
  12. Moffatt, D. L. and K. A. Shubert, “Natural resonances via rational approximants,” *IEEE Trans. Ant. Prop.*, Vol. 25, No. 5, 657–660, 1977.
  13. Kumaresan, R., “On a frequency domain analog of Prony’s method,” *IEEE Trans. on Acoustics, Speech, and Signal Processing*, Vol. 38, Issue 1, 168–170, 1990.
  14. Prony, R., “Essai expérimental et analytique sur les lois de la dilatabilité de fluides élastiques et sur celles de la force expansive de la vapeur de l’alcool à différentes températures,” *J. de l’Ecole Polytechnique*, Vol. 1, Cahier 2, 24–76, Paris, 1795.

15. Sarkar, T. K. and O. Pereira, "Using the matrix pencil method to estimate the parameters of a sum of complex exponentials," *IEEE Ant. and Prop. Mag.*, Vol. 37, No. 1, 48–55, 1995.
16. Wang, S. G., X. P. Guan, X. Y. Ma, D. W. Wang, and Y. Su, "Calculating the poles of complex radar targets," *Journal of Electromagnetic Waves and Applications*, Vol. 20, No. 14, 2065–2076, 2006.
17. Lee, J. H. and H. T. Kim, "Hybrid method for natural frequency extraction: Performance improvement using Newton-Raphson method," *Journal of Electromagnetic Waves and Applications*, Vol. 19, No. 8, 1043–1055, 2005.
18. Rothwell, E., "Natural-mode representation for the field reflected by an inhomogeneous conductor-backed material layer - TE case," *Progress In Electromagnetics Research*, PIER 63, 1–20, 2006.
19. FEKO - EM Software and Systems, [www.feko.info](http://www.feko.info), Technopark-Stellenbosch, South Africa.
20. Berni, A. J., "Target identification by natural resonance estimation," *IEEE Trans. on Aerospace and Electronic Systems*, Vol. AES-11, No. 2, 147–154, 1975.
21. Li, L. and C. H. Liang, "Analysis of resonance and quality factor of antenna and scattering systems using complex frequency method combined with model-based parameter estimation," *Progress In Electromagnetics Research*, PIER 46, 165–188, 2004.
22. Gustafsson, M. and S. Nordebo, "Bandwidth, Q factor, and resonance models of antennas," *Progress In Electromagnetics Research*, PIER 62, 1–20, 2006.
23. Long, Y., "Determination of the natural frequencies for conducting rectangular boxes," *IEEE Trans. Ant. Prop.*, Vol. 42, No. 7, 1016–1021, 1994.
24. Chauveau, J., N. de Beaucoudrey, and J. Saillard, "Characterization of radar targets in resonance domain with a reduced number of natural poles," *EuMW/Eurad*, 69–72, France, Paris, Oct. 2005.
25. Chauveau, J., N. de Beaucoudrey, and J. Saillard, "Analysis of complex shape targets by natural poles of resonance. Determination of characteristic dimensions," *URSI B-279.9*, New Mexico, Albuquerque, July 2006.
26. Toribio, R., "Méthodes d'extraction de pôles de résonance: Application à la caractérisation de cibles," Ph.D. thesis, Université de Nantes, France, 2002.